\



Theoretical study on the exciton dynamics of coherent excitation energy transfer in the phycoerythrin 545 light-harvesting complex

Xue-Yan Cui(崔雪燕), Yi-Jing Yan(严以京), and Jian-Hua Wei(魏建华)

Citation: Chin. Phys. B, 2022, 31 (**1**): 018201. DOI: 10.1088/1674-1056/ac0bad
Journal homepage: http://cpb.iphy.ac.cn; http://iopscience.iop.org/cpb

What follows is a list of articles you may be interested in

Driven injection of a polymer into a spherical cavity: A Langevin dynamics simulation study

Chao Wang(王超), Fan Wu(吴凡), Xiao Yang(杨肖), Ying-Cai Chen(陈英才), and Meng-Bo Luo(罗孟波)
Chin. Phys. B, 2021, 30 (**10**): 108202. DOI: 10.1088/1674-1056/abff21

Multi-phase-field simulation of austenite peritectic solidification based on a ferrite grain

Chao Yang(杨超), Jing Wang(王静), Junsheng Wang(王俊升), Yu Liu(刘瑜), Guomin Han(韩国民), Haifeng Song(宋海峰), and Houbing Huang(黄厚兵)
Chin. Phys. B, 2021, 30 (**1**): 018201. DOI: 10.1088/1674-1056/abc54b

Effect of grain boundary energy anisotropy on grain growth in ZK60 alloy using a 3D phase-field modeling

Yu-Hao Song(宋宇豪), Ming-Tao Wang(王明涛), Jia Ni(倪佳), Jian-Feng Jin(金剑锋), and Ya-Ping Zong(宗亚平)
Chin. Phys. B, 2020, 29 (**12**): 128201. DOI: 10.1088/1674-1056/abad1f

Distribution of a polymer chain between two interconnected spherical cavities

Chao Wang(王超)†, Ying-Cai Chen(陈英才), Shuang Zhang(张爽), Hang-Kai Qi(齐航凯), and Meng-Bo Luo(罗孟波)‡
Chin. Phys. B, 2020, 29 (**10**): 108201. DOI: 10.1088/1674-1056/abaedc

The n-type Si-based materials applied on the front surface of IBC-SHJ solar cells

Jianhui Bao(包建辉), Ke Tao(陶科), Yiren Lin(林苡任), Rui Jia(贾锐), Aimin Liu(刘爱民)
Chin. Phys. B, 2019, 28 (**9**): 098201. DOI: 10.1088/1674-1056/ab33ec

---

Theoretical study on the exciton dynamics of coherent excitation energy transfer in the phycoerythrin 545 light-harvesting complex

Xue-Yan Cui(崔雪燕)[1], Yi-Jing Yan(严以京)[2], and Jian-Hua Wei(魏建华)[1,†]

[1] *Department of Physics & Beijing Key Laboratory of Optoelectronic Functional Materials and Micro-nano Devices, Renmin University of China, Beijing* 100872, *China*

[2] *Hefei National Laboratory for Physical Sciences at the Microscale & Department of Chemical Physics, University of Science and Technology of China, Hefei* 230026, *China*

(Received 6 April 2021; revised manuscript received 27 May 2021; accepted manuscript online 16 June 2021)

The experimental observation of long-lived quantum coherence in the excitation energy transfer (EET) process of the several photosynthetic light-harvesting complexes at low and room temperatures has aroused hot debate. It challenges the common perception in the field of complicated pigment molecular systems and evokes considerable theoretical efforts to seek reasonable explanations. In this work, we investigate the coherent exciton dynamics of the phycoerythrin 545 (PE545) complex. We use the dissipation equation of motion to theoretically investigate the effect of the local pigment vibrations on the population transfer process. The result indicates that the realistic local pigment vibrations do assist the energy transmission. We demonstrate the coherence between different pigment molecules in the PE545 system is an essential ingredient in the EET process among various sites. The coherence makes the excitation energy delocalized, which leads to the redistribution of the excitation among all the chromophores in the steady state. Furthermore, we investigate the effects of the complex high-frequency spectral density function on the exciton dynamics and find that the high-frequency Brownian oscillator model contributes most to the exciton dynamic process. The discussions on the local pigment vibrations of the Brownian oscillator model suggest that the local heterogeneous protein environments and the effects of active vibration modes play a significant role in coherent energy transport.

Keywords: exciton dynamics, light-harvesting complex, quantum coherence

PACS: 82.20.Wt, 82.45.Tv **DOI:** 10.1088/1674-1056/ac0bad

1. Introduction

Photosynthesis is the most important biological process to sustain life on earth. In this process, plants and algae utilize solar energy and convert carbon dioxide into chemical energy. It has aroused researchers interest in understanding the molecular mechanisms, especially under low light conditions, the crucial step in the photosynthesis is to absorb the solar energy, which is captured by the peripheral light-harvesting antenna proteins, and then the energy is transferred to the reaction center where charge separation occurs and stores chemical energy for life.[1–3] Since nature can find the optimum solution, it is unsurprising that excitation energy transfer in the photosynthesis process occurs with high quantum efficiency. Many researchers have investigated the high quantum efficiency of the excitation energy transfer process.[4] The high quantum yield has potential applications in photoelectric conversion devices.

Recently, two-dimensional electronic spectroscopy experiments (2DES)[5–7] reported that long-lived quantum coherence exists in the excitation energy transfer (EET) process of the light-harvesting complex. Collini *et al.*[8] experimentally reported the 2DES of phycoerythrin 545 (PE545) by photon-echo experiments. Moreover, Wong *et al.*[9] investigated the energy transfer process using the two-dimensional electronic spectroscopy method. They observed at least 200 fs quantum beating occurring in the PE545 complex at room temperature. These experimental results lead to a heated debate about the origin of quantum coherence and its effect on excitation energy transfer efficiency.

Recently, reasearchers[10] suggested that the interpretation of small amplitude oscillations in the 2D electronic spectroscopy experiment of photosynthetic complexes needs to be reevaluated. Maiuri *et al.*[11] have carried out a series of transient absorption experiments on the FMO mutants. The experimental results show that the long-lived quantum beat signal is the characteristics of vibrational modes rather than interaction coherence. Thyrhaug *et al.*[12] have investigated the FMO complex by polarization-controlled 2D spectroscopy at low temperatures. They concluded that the quantum beat signal is derived from Raman ground state vibration. These discussions have contributed to the development and understanding of quantum biological systems. Since the coherence in the femtosecond spectroscopy experiment does not represent any subtle quantum effect, the descriptive terms in the discussions of the photosynthesis research require specification.[13] Cao *et al.*[10] suggested that the observation of the long-lived oscillation in the 2D spectroscopy experiment[14] is the focus of the argument for the involvement of interaction coherence or any coherence in the photosynthetic systems. These are inter-

†Corresponding author. E-mail: wjh@ruc.edu.cn

© 2022 Chinese Physical Society and IOP Publishing Ltd

preted as a linear superposition of exciton states, displaying dephasing times of the several hundred femtoseconds. This is considered to be related to the dynamics of energy transfer. However, there are no further detailed experiments and theoretical research using realistic bath parameters to identify coherence signals.

The interpretation of the quantum coherence in the light-harvesting system seems to be controversial. One of the key issues is whether long-lived oscillating coherence is from vibrational modes mainly on the electronic ground state. It is necessary to investigate whether there is long-lived coherence due to pigment-protein vibration when adopting the actual bath parameter. In this work, we investigate the effect of the local pigment-protein vibrations on the exciton dynamic for the PE545 complex. The distribution of vibrational modes enables us to reveal the molecular basis of different spectral density distributions by associating them with modulated bilin intramolecular motion in a protein environment. The actual effect of spectral density comes from the fluctuation of electrostatic pigment-protein interaction associated with a given motion, or from the oscillation of bilin transition energies caused by changes in their internal geometry. The discussion of effect of the coupling between the protein and solvent environment on the exciton dynamic among the chromophores is necessary. We observe the long-lived coherence oscillation in the population transfer process. For the PE545 complex, the results show that the exciton-phonon interactions and vibration of the pigments play an important role in promoting the efficient energy transfer process. The different spectral densities have important implications in the population dynamic of bilin chromophores. It shows that by adopting the spectral densities of the realistic local pigment vibrations one can predict the effects of vibrational dynamics in the coherent exciton dynamic process.

The PE545 pigment-protein complex is extracted from Rhodomonas sp. strain CS24. It can be found in marine and fresh water.[15,16] The bilin chromophores are the primary light-absorbing pigment molecule, which was firstly purified in 1987.[17] The crystal structure of the PE545 complex has been resolved to the resolution of 1.63 Å and 0.97 Å.[18,19] The PE545 complex consists of six phycoerythrobilin (PEB) chromophore molecules and two dihydrobiliverdin (DBV) chromophore molecules.[18] The structural model is illustrated in Fig. 1. The protein scaffold is an $\alpha_1\alpha_2\beta\beta$ heterodimer composed of four subunits indicated as A, B, C and D. Three types of phycoerythrobilins (PEBs) are embedded in each β subunit, namely, $\beta 50/\beta 61$, $\beta 82$, and $\beta 158$. The two additional chromophore molecules related to the subunits α_1 and α_2 are dihydrobiliverdins, DBVs, denoted as $\alpha 19$.[15,20,21] The structure of PE545 pigment-protein enables it to capture the solar energy in low light and to facilitate the excitation energy transfer with a high quantum yield.[8]

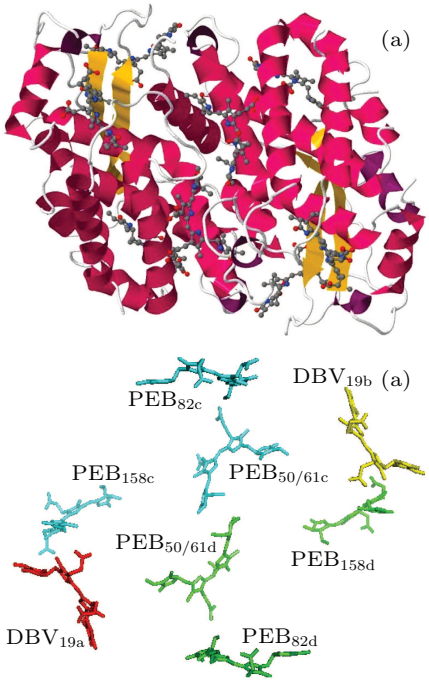


Fig. 1. (a) The structure of PE545 complex with the protein scaffold, eight bilin molecules are embedded in the protein. (b) The eight chromophore molecules from the structural model for the PE545 complex.

The theoretical investigations[20,22–24] have been performed to understand the electronic structures of the chromophore complexes. The electronic properties are often extracted from structure-based calculations or experimental data.[16,24,25] Some structure-based studies used the quantum mechanical/molecular mechanics (QM/MM) methods to describe the environment by the classical polarization force field, which is defined as the QM/MMPol approach.[23,26] The authors employed the MD simulation and QM/MM methods to account for the environmental functions of the local protein scaffold. The environmental effects on the fluctuations of the site energy and electronic coupling were investigated in the PE545 complex.[27] The theoretical research showed that excitation energy transfer efficiency can be improved by dephasing noise due to protein environment vibrations.[28–34] In addition, the very slow protein motions help to increase static disorder to the undisturbed exciton dynamics.[35] The energy transfer process relies on the interactions of excited pigment molecules with their environment. Recent computational chemistry results have shown that the site variations of the spectral density are significant.[36,37] Aghtar *et al.*[38] suggested that the origin of the spectral density of the PE545 complex is from environmental fluctuations. The internal model of the chromophores is essential to the environmental fluctuation. These findings shed light on the possible explanations of the long-lived coherence oscillation. Rivera *et al.*[39] showed that the energy transfer dynamics can be significantly affected by the heterogeneous spectral densities. This may be a mechanism that can

be used to tune the excited energy transfer.

For a long time, it has always been a concerned to understand the mechanism of EET in the photosynthesis system.[40–43] As is known to all, the mechanism of excitation energy transfer is often described as the incoherent hopping mechanism.[44–46] Researchers have recently made some important modifications to the theory, which may give some explanations about the functions of the light-harvesting complexes. Some theoretical results suggest that the general mechanism of environment enhanced excited energy transfer process is the competition between the environment noise enhanced EET process in the weakly dissipative regime and the environment noise-induced suppression in the strongly dissipative regime, this competition results in the efficient energy transfer process.[30,35,47,48] The existence of static disorder decreases the weak dissipation limit and makes the excitation energy transfer process more robust to environmental noise. They offer an interpretation using Fermi's golden rule and find that stochastic resonance enhances the EET process.[47] The design principles for the efficient EET process in these natural light-harvesting complexes would have great significant implications to design the efficient synthetic devices.[47,49] These researches inspire us in the design of artificial chemical systems that can be applied in sensors, photon conversion, and organic solar cells.[50,51]

In this article, we report the investigations on the exciton dynamics of the PE545 complex. To investigate the effect of the vibration of pigment-protein complexes, we use the spectral density of individual pigment molecules to perform the numerical calculation of the population dynamics in the PE545 complex. The results suggest that spectral density properties of the exciton-phonon interactions can be the basis for effective excitation energy distribution in the PE545. We observe that the coherent exciton dynamics can be affected by the heterogeneous spectral densities. The population dynamics rely on the interactions between excited pigment molecules and their environment. We use the dissipation equation of motion (DEOM) to theoretically investigate the effects of heterogeneous spectral density modes on the exciton dynamics in the PE545 antenna complex.

2. Model and theory

To elucidate the exciton dynamic of the PE545 complex, an exciton model is established by the full Hamiltonian which is obtained from structure calculation.[21,22] The electronic coupling calculations are based on the transition dipole moment obtained from quantum mechanical/molecular mechanics (QM/MM) methods.[16,23] The structure of the PE545 complex is characterized by the large average center distance of bilin chromophores. As described by Curutchet *et al.*,[52] they calculated the transition dipole moment of each chromophore and electronic coupling between the bilins by the CIS/6-31G method.[52–54] The results include the screening of the Coulomb coupling by the polarizable surrounding adopting the polarizable continuum (PCM) model.[55] Researchers[16] proposed the exciton model based on the simultaneous fit of steady-state spectra responses of the PE545 complex. The exciton Hamiltonian of the PE545 is listed in Table 1.

Table 1. The site energies and the electronic coupling elements between pigments of the PE545 complex (in cm^{-1}).[16]

Site	1	2	3	4	5	6	7	8
DBV19a	18008	–4.1	–31.9	2.8	2.1	–37.1	–10.5	45.9
DBV19b	–4.1	17973	–2.9	30.9	–35.4	2.5	–45.5	11.0
PEB158c	–31.9	–2.9	18711	–5.6	–19.6	–16.1	6.7	6.8
PEB158d	2.8	30.9	–5.6	18960	11.5	25.5	5.1	7.4
PEB50/61c	2.1	–35.4	–19.6	11.5	18532	101.5	36.3	16.0
PEB50/61d	–37.1	2.5	–16.1	25.5	101.5	19574	17.6	–38.6
PEB82c	–10.5	–45.5	6.7	5.1	36.3	17.6	18040	2.6
PEB82d	45.9	11.0	6.8	7.4	16.0	–38.6	2.6	19050

The functional role of this interacting multi-chromophore system can be formed by the Hamiltonian consisting of H_s, H_b and H_{sb}. The PE545 complex has the quantum subsystem components, H_s, which contains only the system operator, and the system-bath coupling component, H_{sb}, which includes both system and bath quantity. Because the excitation pigment molecules are delocalized, we represent the total Hamiltonian in terms of the Frenkel exciton model. Thus the total Hamiltonian can be expressed as $H_{tot} = H_s + H_b + H_{sb}$. The PE545 electronic states are modeled as an eight-level quantum system with Hamiltonian

$$H_s = \sum_{j=1}^{N} \varepsilon_j |j\rangle\langle j| + \sum_{j\neq k}^{N} J_{jk} |j\rangle\langle k|, \tag{1}$$

where $|j\rangle$ denotes the excited state of the chromophore spatially located at the site j. The diagonal site energy is represented by ε_j. The intensity of the dipole-dipole interaction between pigments in different sites can be expressed by J_{jk}. We model the protein environment as a set of harmonic oscillators with $H_b = \sum_\alpha \hbar\omega b_\alpha^\dagger b_\alpha$. Each pigment molecule is coupled to the bath via the interaction Hamiltonian $H_{sb} = S_j B_j$, with

$S_j = |j\rangle\langle j|$, where B_j is the bath operator.

We adopt the bath correlation function $C(t)$ that is a Drude–Lorentzian correlation function. It is concerned with the environment spectral density $J(\omega)$ by the fluctuation-dissipation theorem, given as[56]

$$\begin{aligned} C_j(t) &= \langle \tilde{B}_j(t)\tilde{B}_j(0)\rangle \\ &= \frac{1}{\pi}\int_{-\infty}^{\infty} \mathrm{d}\omega J(\omega)\frac{\exp(-\mathrm{i}\omega t)}{1-\exp(-\hbar\omega/k_{\mathrm{B}}T)}, \end{aligned} \tag{2}$$

where the form of system-bath interaction is characterized as $J(\omega) = (\pi/2)\sum_j c_j^2\delta(\omega-\omega_j)$.[57] In this work, the population dynamic of the system and bath is simulated by the DEOM theory.[58–60] The DEOM method is one of the most important methods to study the open quantum system. Recently, Yan *et al.*[61,62] have proposed the Fano spectrum decomposition scheme (FSD) at near-zero temperatures. The method has good applicability at low temperatures. It can overcome the discontinuity of Fermi or Bose function at near-zero temperature. They indicated that the FSD scheme converges fast at low temperatures. It is of great value to the effective numerical calculation in various low temperatures condensed physics problems. The DEOM method not only recovers the HEOM method but also identifies the physical significance of the involved dynamical quantity as many dissipation configurations. As a "second-quantization" theory of the HEOM formalism,[63,64] many unique features of the DEOM method are beyond the reach of the HEOM framework. The DEOM theory includes not only the rule of dynamics of the evolution variables but also the law of the underlying statistical quasi-particle and novel dissipative algebras. Particularly, Wick's theorem provides the DEOM with a general means for evaluating various experimental measurable quantities of the system and bath interference dynamic.[58] The DEOM approach provides a statistical quasi-particle picture to explain the environment, which can be bosonic or fermionic. In this sense, the DEOM method is a second-quantization theory of the open system. The theory of the dissipation equations of motion adopts a general form of the system Hamiltonian. It applies to a wide range of system parameters without additional derivation and programming efforts. The DEOM approach is non-perturbative. It treats the hybrid environment dynamic from the perspective of open quantum dissipative dynamic. In principle, the DEOM method is formally accurate for the linear hybridization bath. Physically, the DEOM can describe both the system and hybrid bath dynamic. Mathematically, it forms a linear space that gives rise to all the standard prescriptions of quantum mechanics. The DEOM method is recently developed by Yan *et al.*[59] The dynamic variables in the DEOM are called dissipation density operators, and their general form is as follows:[60,65]

$$\rho_n^{(n)}(t) \equiv \rho_{n_1,\ldots,n_K}^{(n)}(t) \equiv \mathrm{tr}_{\mathrm{B}}[(\hat{f}_1^{n_1},\ldots,\hat{f}_K^{n_K})^{\circ}\rho_{\mathrm{T}}(t)]. \tag{3}$$

The dissipations inside the circled parentheses, $(,\ldots,)^{\circ}$, are irreducible, which satisfy the bosonic permutation relation $(\hat{f}_k,\ldots,\hat{f}_{k'})^{\circ} = (\hat{f}_{k'},\ldots,\hat{f}_k)^{\circ}$. In Eq. (3), $n = n_1+\cdots+n_k$, with $n_k \geq 0$ being the participation number of the specified dissipation and $n \equiv \{n_1,\ldots,n_K\}$. They specify the composite of the n-dissipation cluster, $\rho_n^{(n)}$ of Eq. (3). The $(n+1)$-dissipations are characterized by $\rho_{n_k^{\pm}}^{(n\pm1)}$. The DEOM formalism can be represented as the general formalism

$$\dot{\rho}_n^{(n)} = -[\mathrm{i}\mathcal{L}+\gamma_n^{(n)}]\rho_n^{(n)} + \{\rho_{n^-}^{(n-1)}\} + \{\rho_{n^+}^{(n+1)}\}. \tag{4}$$

It is constructed by the application of the quantum Liouville equation $\dot{\rho}_{\mathrm{T}}(t) = -\mathrm{i}[H_{\mathrm{s}}+H_{\mathrm{b}}+H_{\mathrm{sb}},\rho_{\mathrm{T}}(t)]$ for the total density operator in Eq. (3). The $\mathcal{L}$ is the definition of system Liouvillian superoperator, in general, the system Hamiltonian gives rise to $\mathcal{L}$ of $\mathcal{L}\cdot \equiv [H,\cdot]$, the H_{b} term is evaluated by the generalized diffusion equation and the H_{sb} commutator is evaluated by the generalized Wick's theorem. This theoretical method gives numerically exact results and verifies the long-lived coherence dynamic in the PE545 complex at low temperature and room temperature, respectively. The method is also reliable to explore the effect of the system-environment coupling strengths on the exciton dynamic process between chromophores, in addition, it can provide numerical results on the coherence density matrix elements. The numerical results are beneficial for us to understand the exciton dynamics in the PE545 network.

For the PE545 complex, we use the spectral density function in the Drude regularized Ohmic form of

$$J(\omega) = 2\lambda\gamma\omega/(\omega^2+\gamma^2). \tag{5}$$

Wong *et al.*[9] conducted spectroscopy experiments to provide the adiabaticity description of the free energy in the PE545 complex, and they adopted the spectral density parameters which are the reorganization energy of $\lambda = 110\ \mathrm{cm}^{-1}$ and bath cutoff frequency $\gamma = 19.176\ \mathrm{cm}^{-1}$ to obtain the agreement between the experimental data and numerical fitting. Thus, we employ these parameters to calculate the population dynamics in the PE545. The results show that the electronic coherence time is consistent with the observed results by Wong *et al.* with 2D electronic spectroscopy.[9] The spectral function is a key feature describing the excitation dynamics in an open quantum system. We also discuss the influence of different spectral density functions on the coherent exciton dynamic process, and we consider the high-frequency Brownian oscillator model[56,66]

$$J(\omega) = \frac{2\lambda}{\pi}\frac{v\Omega^2\omega}{(\Omega^2-\omega^2)^2+v^2\omega^2}. \tag{6}$$

It corresponds to the spectral density of a set of damped harmonic oscillators of reorganization energy λ, frequency Ω with associated damping v. We present the calculation results of the model by the DEOM method.

3. Results and discussion

Experimentally, the quantum coherence in the PE545 complex can be observed by the two-dimensional electronic spectroscopy method.[9] It was observed that the long-lived quantum coherence exists. In this work, we investigate the coherence exciton dynamic process in the PE545 complex using the DEOM method. We adopt the Drude spectrum to describe the environmental spectral density, with the reorganization energy[9] $\lambda = 110$ cm^{-1} and the cutoff frequency $\gamma = 19.176$ cm^{-1}. The parameters of the spectral densities are derived from the numerical fitting of the experiment data. In addition, the spectral density is equivalent for each bilin. We present the results of the PE545 complex in Fig. 2. The calculated results are in agreement with the experimental observations. Since DBV19b chromophore molecules are adjacent to the PEB82c pigment molecules on the protein structure scaffold and the electronic coupling energy (-45.5 cm^{-1}) between the DBV19b and PEB82c sites is strong, when the DBV19b pigment molecule is initially excited, we observe that the population of the DBV19b and PEB82c pigment molecules appear a coherent oscillation phenomenon. As shown in Fig. 2(a), it is remarkable that coherence time lasts up to ~ 600 fs at low temperature, and in Fig. 2(b), electronic coherence persists for about 400 fs after excitation at room temperature. Our calculation results of the PE545 complex are in good agreement with the experimental results of Wong *et al.*[9] with two-dimensional electronic spectroscopy.

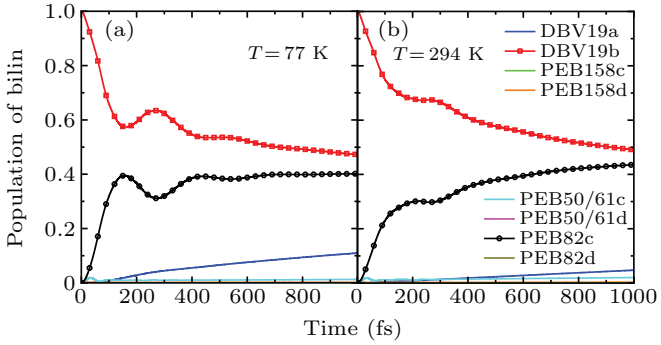


Fig. 2. Population dynamics of the eight bilins model at $T = 77$ K and $T = 294$ K, the reorganization energy $\lambda = 110$ cm^{-1} and the cut-off frequency $\gamma = 19.176$ cm^{-1}, respectively.

Furthermore, we have calculated the population dynamic with excitons initially located at other pigments to study the excitation energy transfer pathway. When the PEB82c or PEB158c pigment molecule is initially excited, as shown in Fig. 3, we observe the differences among the individual pigment population dynamics. In the case of initially exciting the PEB82c pigment molecule, the phenomenon of coherence occurs. Subsequently, the excitation more quickly migrates to the DBV19a chromophore molecule (shown by blue line). At about 10 ps, the population of the DBV19a bilin slightly exceeds the population of the initially excited PEB82c pigment molecule. When initially exciting the PEB158c pigment, the excitation energy is first transferred to the PEB50/61c molecule. As time increases, the populations accumulated on PEB82c and DBV19a chromophore gradually increase. Eventually, the population flows to the DBV19a chromophore molecule. The efficient excitation energy transfer pathway on the EET process is that the PEBs absorb the solar energy and transfer the energy to the DBVs chromophores. By taking different initial excitation, significantly affects the redistribution of the population and the time scale in the EET process.

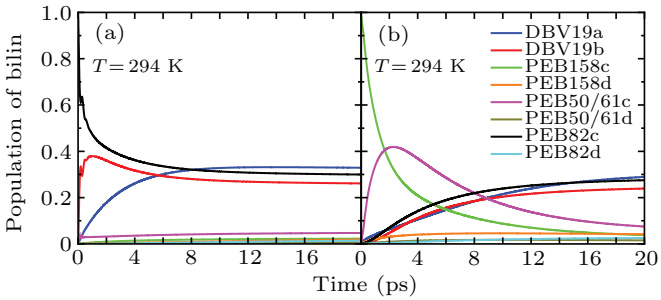


Fig. 3. The site population dynamics of the PE545 complex at $T = 294$ K with initial excitation on PEB82c and PEB158c chromophores, respectively.

To discuss the effect of system-bath coupling strength on the exciton dynamics process between chromophore molecules in the PE545 network, we performed a series of calculations, in which we changed the solvent reorganization energy with the Drude spectral density at room temperature. We present the time-dependent site population dynamic results for different chromophores in Fig. 4. The ubiquitous behaviors observed on the panels of this figure show an optimization of the population within the coherent time scale by changing reorganization energy parameter values in multiples of $\lambda = 110$ cm^{-1}. When the DBV19b pigment molecule is initially excited, as shown in Fig. 4(a), the population oscillating for reorganization energy λ, arrives at about 0.6 at $t = 400$ fs. As shown by the red line and green line, with the increase of the reorganization energy, such as 2λ, 3λ,..., the value of the population of this state is larger than that of λ. For the larger reorganization energy values, (e.g., 6λ and 7λ), the population value of this initial excited state increases with increased coupling strength to the environments. Therefore, this exciton state is found to be optimal at about λ.

In Figs. 4(b)–4(d), the populations of other chromophores show a trend of maximization with different reorganization energies. For instance, as shown in Fig. 4(b), we observe that the population of the DBV19a chromophore decreases as the solvent reorganization energy increases to 7λ. In addition, the value of the population decreases by about a factor of 5 as the reorganization energy increases to 7λ. Based on the location of these chromophores in the network, different chromophores

exhibit the maximization of the population under different values of the reorganization energy. For example, the PEB82c chromophore (in Fig. 4(c)) shows population oscillation under different intensities of coupling between the system and the environment. The value of population maximizes at the low values of reorganization energy around λ. The behavior of population oscillation for the PEB158d pigment molecule is asymptotic as shown in Fig. 4(d). We observe the maximum value of the population at a larger solvent reorganization energy 6λ.

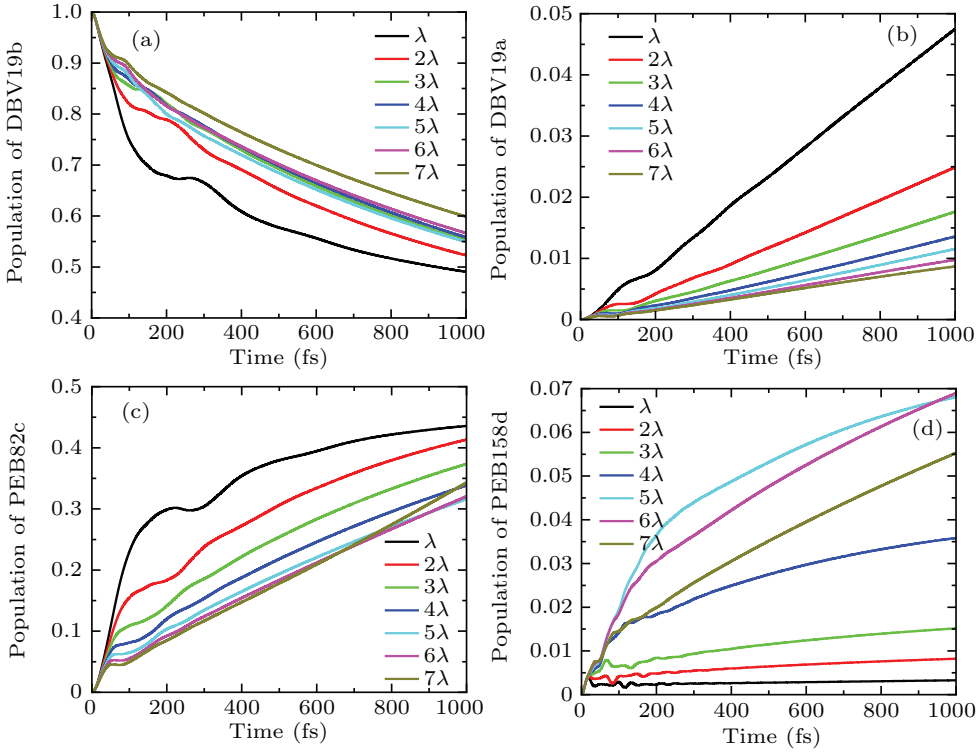


Fig. 4. Population dynamics of different pigment states with time evolution after initial excitation on the DBV19b site. Each panel shows the results of the different chromophore in the networks and discusses the effect of the coupling strength between the system and bath characterized by the parameter of solvent reorganization energy λ on the site population dynamic.

The optimization behavior that increases the coupling strength of the system bath is observed in the simple model of the light-harvesting networks.[30,67] We use stochastic resonance to reveal this behavior. When the system-bath coupling changes, the population of the chromophore will be affected. As the fluctuation of the site energies becomes on the order of the electronic excitation energy gaps, the resonate between the fluctuation of the site energies and excitation energy will happen many times. With the stronger system–bath coupling, the larger fluctuations of the site energy drive the systems out of resonance. We observe that a decrease in population transport in the light-harvesting network. As a matter of fact, the results in Fig. 4 reveal these characteristics of the stochastic resonance behavior.

Theoretically, the study of exciton dynamics in the dissipative environment can be carried out by the dissipation equation of motion formalism, but a detailed understanding of the spectral density of quantized exciton-phonon interaction is needed. Recently, researchers have used the combined classical molecular dynamics (MD) and QM/MMPol methodology to study the exciton–phonon interaction in the PE545 complex.[37] They reported the resulting spectral density averaged over all pigments based on the spectroscopy studies. The reorganization energy is associated with the spectral density by the relation $\lambda = \int_0^\infty \frac{J(\omega)}{\omega} \mathrm{d}\omega$. For the Drude spectral density, the parameter values of the spectral density are reorganization energy $\lambda = 24.14$ cm^{-1} and cutoff frequency $\gamma = 56.82$ cm^{-1}.[37] Then we use the DEOM theory to investigate the effect of exciton-phonon interaction on the population dynamic. We calculate the exciton population dynamics, which show coherence oscillation lasting up to 800 fs at $T = 77$ K as shown in Fig. 5(a). When the initial excitation is on the DBVb pigment molecule at $T = 294$ K, the electronic coherence time is about 500 fs in Fig. 5(b), there is a longer coherence time at low temperature, which is helpful to the exciton dynamics process.

We confirm that the oscillations of exciton dynamic between different sites are interpreted as coherence. Moreover, the disappearance of this oscillation is explained by the loss of coherence. It seems that the coherence only exists on the time scale where the oscillation persists, however, such time scale only accounts for a few percentages of the entire exciton dynamic process of the PE545 complex. We discuss the roles of coherence on the exciton dynamic process, and to what extent

does coherence affects the dynamic process. It is important to investigate whether the exciton dynamic remains coherent, even after the excitation oscillations stop. By detailed calculations, we have demonstrated the roles of coherence in this part. We believe that coherence plays an independent role in the exciton dynamic. Note that the diagonal or coherence density matrix elements represent the population, which describes the probability that the ith chromophore site is excited, but the off-diagonal decoherence elements of the density matrix, which represent the coherences between the ith and jth chromophore sites. By using the parameters of spectral density[37] with reorganization energy $\lambda = 24.14$ cm^{-1} and cutoff frequency $\gamma = 56.82$ cm^{-1}, we calculate the population dynamics in the PE545 complex.

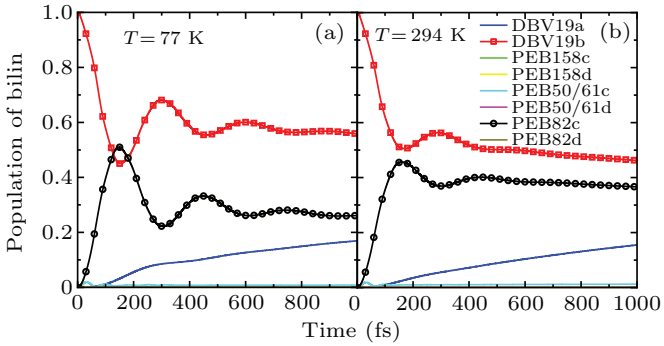


Fig. 5. Site population dynamics of the eight sites model at $T = 77$ K and $T = 294$ K, the reorganization energy $\lambda = 24.14$ cm^{-1} and the cutoff frequency $\gamma = 56.82$ cm^{-1}, respectively.

As shown in Fig. 6, we present the dynamic calculation results of the absolute value of the main off-diagonal elements of the density matrix in the site basis. The off-diagonal elements of the density matrix are identified as the oscillation of excitation, and the dynamical behaviors of the off-diagonal density matrix elements give decoherence time scales. The relaxation time of the amplitude of the off-diagonal density matrix element calculated in the site basis provides a reasonable estimation of the decoherence time obtained in the photon-echo experiment.[9] When initially excited on the DBV19b site at room temperature, we observe that the excitation oscillation process achieving the steady-state on a time scale of about 300 fs. Generally, in the dynamics of the PE545 complex, the population oscillation is regarded as the signature of coherence. This means that once the oscillation of excitation no longer exists, the coherence should be disappeared. However, our dynamical calculation results reveal that the time scale of coherence lasts for a longer time than the excitation energy oscillation, which is on the time scale of about 500 fs as shown in Fig. 5(b). By calculating the main off-diagonal elements of the density matrix terms, we find that the role of coherence cannot be ignored. It is the basic component of exciton dynamics between different sites. Therefore, it is invalid to say that coherence only exists on the time scale of the excitation oscillation, on the contrary, it also exists for the time when the excitation no longer oscillates. It implies that the coherences play an important and independent role in the exciton dynamics process in the PE545 complex.

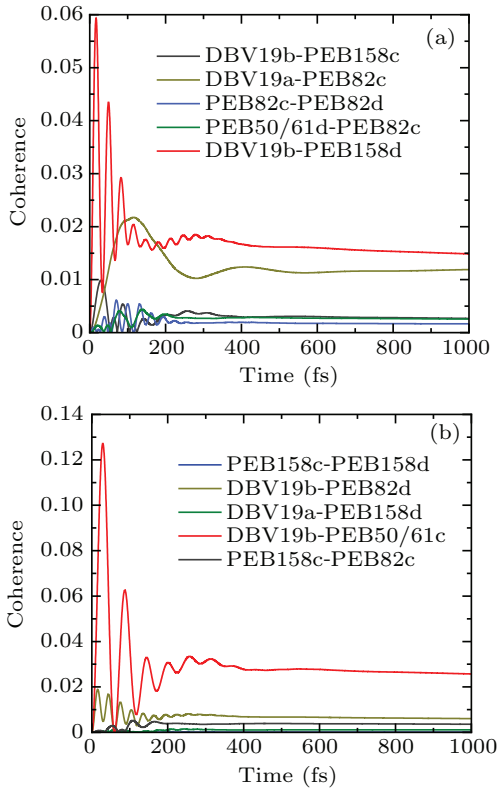


Fig. 6. Temporal evolution of off-diagonal coherence density matrix elements plotted as $|\rho_{ij}^{\text{site}}|$ in the site representation for the PE545 complex at $T = 294$ K.

In reality, because the local protein environments translate into slightly different characteristics of the spectral density of each pigment, and the interaction between each chromophore molecule and its surrounding protein environment is also diverse, the spectral density of each pigment molecule is different. From the quantum chemistry and molecular dynamics calculations,[37] we can adopt the site-varying spectral densities to investigate the population dynamic process. The computed values[37] of the reorganization energy and cutoff frequencies are presented in Table 2. The PE545 complex has a fairly important range of λ values, in which the maximum of the reorganization energy value is larger than 5 times the minimum. As shown in the table, the average reorganization energy value from Table 2 is about 15 cm^{-1}, the average reorganization energy is also the most representative in a sense because the reorganization energy value of half of the pigments is close to this value. When compared with the PEBs pigment, the DBVs sites have larger reorganization energies around 26 cm^{-1}. Among the PEBs pigment molecules, the PEB158 pairs have the largest system-bath coupling, followed by the PEB50/61 pairs and PEB82 pairs featuring reorganization energies λ values of ~ 15, ~ 12, and ~ 6 cm^{-1}, respectively. The difference in reorganization energies is considered

to play an important role in the population dynamics of the PE545 complex, as discussed below.

Table 2. Values of the PE545 complex Drude–Lorentz spectral density for the individual pigments,[37] site-dependent model reorganization energies λ and cutoff frequencies γ used in this work.

m	λ (cm^{-1})	γ (cm^{-1})
DBV19a	25.58	42.76
DBV19b	27.32	36.82
PEB158c	15.47	25.43
PEB158d	15.51	32.74
PEB50/61c	11.70	20.51
PEB50/61d	12.62	16.78
PEB82c	5.41	18.65
PEB82d	7.54	18.98

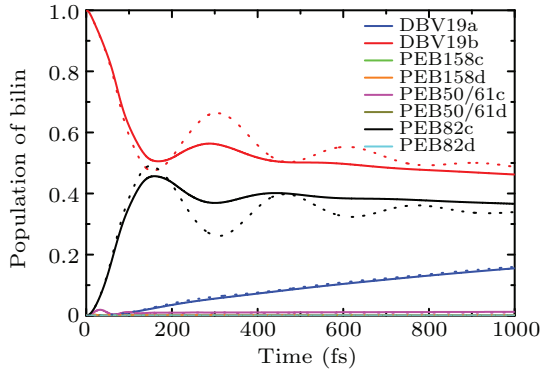


Fig. 7. Comparison of the identical spectral density configuration $\lambda = 24.14$ cm^{-1} and $\gamma = 56.82$ cm^{-1} (solid curves) with site-dependent of λ and γ (dashed curves), with initially excited on DBV19b chromophore at $T = 294$ K.

In Fig. , we present the dynamic results in the two different spectral densities model. One is the site-dependent spectral density model, which includes the interaction effect between each pigment molecule and its surrounding environment. Another one is the site-independent spectral densities model, which shares the same spectral density for each pigment. The Drude–Lorentz spectral density is used to calculate the effect of the site-dependent model on the exciton dynamics. The parameters of the site-dependent spectral density are listed in Table 2. For the site-independent spectral densities model, we use the reorganization energy $\lambda = 24.14$ cm^{-1} and cutoff frequency $\gamma = 56.82$ cm^{-1} to calculate the exciton dynamic. We compare the calculated results using the site-dependent spectral density model with that of the site-independent spectral density model. The population dynamics show the difference between the site-independent spectral densities model (solid curve) and the site-varying of λ and γ (dashed curve). It is observed that the population coherent oscillation time scale is much longer than that with the site-independence spectral density model. The results show a longer-lived coherence oscillation in the site-dependent spectral densities model, so we can partially optimize the mode of site-dependent spectral densities to accelerate the dynamics process.

The spectral density we present is a relatively simple low-frequency Drude–Lorentz Ohmic form, which is only characterized by two physical bath parameters. We believe that the simplified spectral density form may not deeply explain the exciton dynamic process of the PE545 complex. Therefore, we also use the high-frequency Brownian oscillator model to calculate the population dynamics. For the Brownian oscillator model, we adopt the values[37] of reorganization energy $\lambda = 18.144$ cm^{-1}, frequency $\Omega = 199.256$ cm^{-1}, with associated damping $v = 93.709$ cm^{-1}. These parameter values are based on the theoretical calculation by the overall average spectral density of all pigment molecules. As shown in Fig. 8, when the DBV19b chromophore is initially excited, we present the population dynamic results at room temperature. We observe that the population of DBV19b and PEB82c sites show the phenomenon of coherent oscillation, and the coherence time lasts for about 800 fs. From the results of dynamics calculation, there is a relatively long-lived coherence time in the PE545 complex using the Brownian oscillator spectral density model.

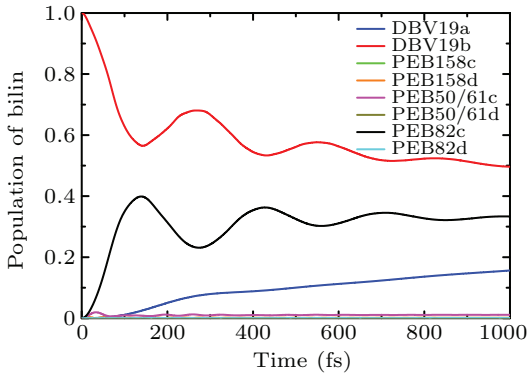


Fig. 8. The site population dynamics of the eight sites model at $T = 294$ K, adopting the high frequency Brownian oscillator (BO) model of the PE545 complex, with the reorganization energies λ, frequency Ω and associated damping v.

Table 3. Values of the PE545 complex Brownian oscillators (BO) spectral density for each chromophore,[37] with the reorganization energies λ, frequency Ω and associated damping v.

m	λ (cm^{-1})	Ω (cm^{-1})	v (cm^{-1})
DBV19a	4.628	89.913	54.56
DBV19b	10.376	110.255	64.92
PEB158c	18.853	94.272	109.625
PEB158d	16.85	82.914	71.733
PEB50/61c	3.872	63.018	45.191
PEB50/61d	7.627	82.585	67.183
PEB82c	6.698	50.224	40.443
PEB82d	9.055	87.19	110.143

To discuss the effect of local pigment-protein vibration on exciton dynamic for individual bilin chromophore, we use the realistic site variations spectral densities of the Brownian oscillator model to describe the interactions of the excited molecules with their nuclear vibrational environment. From the molecular dynamics and quantum chemistry

calculations,[37] the parameters of the BO spectral density for each chromophore are listed in Table 3. We use the site-varying spectral densities to investigate the exciton dynamics. In Fig. 9, we present the population dynamic results by the site-varying Brownian oscillator spectral densities model. We observe that the intensity of the amplitude and the frequency of the coherence oscillation are relatively robust. We use spectral density which is the characterization of exciton-phonon interactions to simulate the population dynamic process. The population dynamic results show that the coherent oscillation time is about 1000 fs, this coherence time is longer than that of the BO spectral density model in which each chromophore has the same spectral density. The result shows that the realistic local vibration spectral density model is conducive to modulate the dynamic in the PE545 complex. The vibrational modes induced by the pigment-protein environment vibrations have a significant impact on the exciton dynamics process.

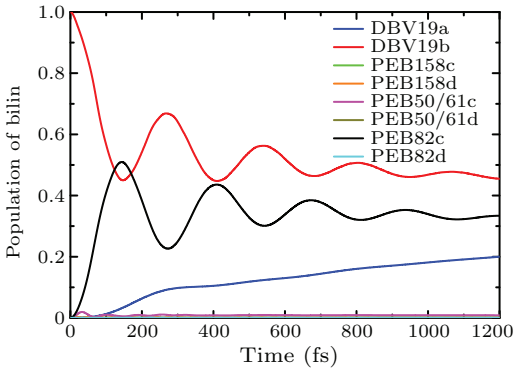


Fig. 9. The populations dynamic with Brownian oscillator (BO) spectral density for each chromophore at $T = 294$ K, in which the initially excited on the DBV19b pigment molecule.

To compare the effects of the low-frequency and high-frequency spectral densities on the exciton dynamics, we calculated the population dynamics of the PE545 complex with two different spectral densities at 294 K. The low-frequency spectral density model is Drude form, where the reorganization energy is 24.14 cm^{-1} and cutoff frequency is 56.82 cm^{-1}. On the other hand, we also calculated the exciton dynamic in the PE545 complex when the spectral density function is the high-frequency Brownian oscillator (BO) model. As illustrated in Fig. 10, we show the results of the quantum coherence dynamics process in the PE545 complex. The solid line represents the dynamic result of the Drude spectral density, and the dashed line represents the result of the time evolution of the Brownian oscillator spectrum model. The population coherent oscillations last for more than 800 fs in the case of the Brownian oscillator spectral density model. The results indicate that the BO spectrum function leads to the longer-lived coherence for DBV19b and PEB82c molecules, which means that the BO spectrum density model is more conducive to the exciton dynamic process.

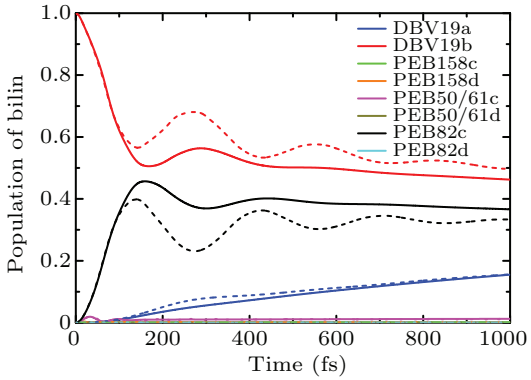


Fig. 10. The comparison of populations with different spectral density models at $T = 294$ K, computed with the Drude–Lorentz spectral density (solid curves) and Brownian oscillator model (dashed curves).

4. Conclusion

In summary, we have theoretically investigated the population dynamics of the PE545 light-harvesting complex in detail. We use the Drude spectral density form, with the parameters of reorganization energy $\lambda = 110$ cm^{-1} and the cutoff frequency $\gamma = 19.176$ cm^{-1}. The results reveal that the presence of coherence motion can persist for about 400 fs even at room temperature, which is consistent with the experimental results. In the meantime, we also calculate the population dynamics among the individual chromophores to study the energy transfer pathway. The excitation energy transfer pathway is that the PEB chromophores absorb the solar energy and transfer the excited energy to the DBV chromophores. We investigate the influence of the strength of the system-bath coupling on the population dynamic process of the PE545 complex and perform a series of exciton dynamics calculations. We believe that a certain optimal value is conducive to the dynamics process for individual chromophores. This observation indicates that the local protein environment around the pigment molecules may be adjusted in a controllable way to affect network throughput. The insights can help us to design artificial light-harvesting complex and provide design principles for photovoltaic electronic devices.

For the PE545 complex, to analyze the explicit roles of the coherence in the excitation energy delocalization process, we perform numerical calculations with reorganization energy $\lambda = 24.14$ cm^{-1} and the cutoff frequency $\gamma = 56.82$ cm^{-1} at room temperature. The quantum coherent beating signals are observed and the coherence time is about 500 fs. We display the population dynamic results of the absolute value of the main off-diagonal elements of the density matrix in the site basis, where we observe the oscillation up to about 300 fs. The population oscillation is considered as the signature of coherence, and the off-diagonal elements of the density matrix are regarded as the oscillation of excitation. The dynamical calculation results show that the time of the coherence beating lasts for a longer time than the excitation oscillation. As a general

comment, it implies that the coherence and therefore the delocalization process is an essential component for the population redistribution among the chromophores. It essentially means that coherence plays an equivalently important and independent role in the dynamics process.

In general, quite a few simulations have been performed, which focus on the PE545 complex. Because structures of pigment molecules and the interactions with the surrounding environment are different, the fluctuation of the protein environment around the individual pigment molecule will affect the spectral density distribution of each chromophore. To investigate the effects of the different spectral density models on the exciton dynamics process, we have performed a series of population dynamic calculations with the local heterogeneous protein environment. We compare the calculation results between the heterogeneous protein environment (site-dependent spectral density) and the identical spectral density model (site-independent spectral density). The results reveal that the models of the local heterogeneous protein environment have longer-lived quantum coherence compared with the homogeneous environment. Consequently, the local protein environment fluctuations of each pigment molecule play an important role in the dynamic process.

Since the spectral density we used is the Drude–Lorentz form, which is only characterized by the reorganization energy and cutoff frequency. We believe that such a spectral density function is slightly simple to elucidate the exciton dynamic. Thus, we adopt the complicated Brownian oscillator model to study the dynamic process. Comparing the calculated results of these two types of spectral densities indicates that Brownian oscillator spectrum function models have longer-lived coherence time. Thus, we realize that the Brownian oscillation model plays an important role in the population dynamics process. By the local pigment vibrations of the Brownian oscillator model, we believe that the realistic local vibration spectral density model is conducive to modulate the exciton dynamic process in the PE545 complex. In conclusion, these results indicate that the local pigment-protein vibration for each chromophore can significantly affect the dynamics process, which may provide applications in designing highly efficient artificial photosynthesis systems.

Acknowledgements

This work was supported by the Natural Science Foundation of China (Grant Nos. 11774418 and 11374363). The computing resources are provided by the High Performance Computing Physics Laboratory at Renmin University of China.

References

[1] Novoderezhkin V I and Grondelle R V 2010 *Phys. Chem. Chem. Phys.* **12** 7352
[2] Blankenship R E 2014 *Molecular Mechanisms of Photosynthesis* (Chichester: John Wiley and Sons) pp. 3–10
[3] Hu X, Ritz T, Damjanovic A, Autenrieth F and Schulten K 2002 *Q. Rev. Biophys.* **35** 1
[4] Wang X L, Li H R, Zhang P and Li F L 2013 *Chin. Phys. B* **11** 117102
[5] West B A and Moran A M 2012 *J. Phys. Chem. Lett.* **3** 2575
[6] Jonas D M 2003 *Annu. Rev. Phys. Chem.* **54** 425
[7] Brixner T, Stenger J, Vaswani H M, Cho M, Blankenship R E and Fleming G R 2005 *Nature* **434** 625
[8] Collini E, Wong C Y, Wilk K E, Curmi P MG, Brumer P and Scholes G D 2010 *Nature* **463** 644
[9] Wong C Y, Alvey R M, Turner D B, Wilk K E, Bryant D A, Curmi P MG, Silbey R J and Scholes G D 2012 *Nat. Chem.* **4** 396
[10] Cao J S, Cogdell R J, Coker D F *et al.* 2020 *Sci. Adv.* **6** eaaz4888
[11] Maiuri M, Ostroumov E E, Saer R G, Blankenship R E and Scholes G D 2018 *Nat. Chem.* **10** 177
[12] Thyrhaug E, Tempelaar R, Alcocer M J P, Žídek K, Bína D, Knoester J, Jansen T L C and Zigmantas D 2018 *Nat. Chem.* **10** 780
[13] Mancal T 2020 *Chem. Phys.* **532** 110663
[14] Engel G S, Calhoun T R, Read E L, Ahn T K, Mančal T, Cheng Y C, Blankenship R E and Fleming G R 2007 *Nature* **446** 782
[15] Doust A B, Van S I H M, Larsen D S, Wilk K E, Curmi P M G, Van G R and Scholes G D 2005 *J. Phys. Chem. B* **109** 14219
[16] Hossein N H, Curutchet C, Kubica A and Scholes G D 2011 *J. Phys. Chem. B* **115** 5243
[17] Hiller R G and Martin C D 1987 *BBA Gen. Subj.* **923** 98
[18] Wilk K E, Harrop S J, Jankova L, Edler D, Keenan G, Sharples F, Hiller R G and Curmi P M G 1999 *Proc. Natl. Acad. Sci. USA* **96** 8901
[19] Doust A B, Marai C N J, Harrop S J, Wilk K E, Curmi P M G and Scholes G D 2004 *J. Mol. Biol.* **344** 135
[20] Curutchet C, Novoderezhkin V I, Kongsted J, Losa M A, Grondelle R V, Scholes G D and Mennucci B 2013 *J. Phys. Chem. B* **117** 4263
[21] Novoderezhkin V I, Doust A B, Curutchet C, Scholes G D and Grondelle R V 2010 *Biophys. J.* **99** 344
[22] Tong Z Q, Huai Z, Mei Y and Mo Y 2020 *J. Chem. Phys.* **152** 135101
[23] Tong Z Q, Huai Z, Mei Y and Mo Y 2019 *J. Phys. Chem. B* **123** 2040
[24] Curutchet C, Kongsted J, Losa M A, Nejad H H, Scholes G D and Mennucci B 2011 *J. Am. Chem. Soc.* **133** 3078
[25] Viani L, Curutchet C and Mennucci B 2013 *J. Phys. Chem. Lett.* **4** 372
[26] Chandrasekaran S, Pothula K R and Kleinekathöfer U 2017 *J. Phys. Chem. B* **121** 3228
[27] Aghtar M, Kleinekathöfer U, Curutchet C and Mennucci B 2017 *J. Phys. Chem. B* **121** 1330
[28] Fleming G R, Scholes G D and Cheng Y C 2011 *Procedia. Chem.* **3** 38
[29] Rebentrost P, Mohseni M, Kassal I, Lloyd S and Guzik A A 2009 *New J. Phys.* **11** 033003
[30] Plenio M B and Huelga S F 2008 *New J. Phys.* **10** 113019
[31] Caruso F, Chin A W, Datta A, Huelga S F and Plenio M B 2009 *J. Chem. Phys.* **131** 105106
[32] Mohseni M, Rebentrost P, Lloyd S and Guzik A A 2008 *J. Chem. Phys.* **129** 174106
[33] Chen H, Wang X, Fang A P and Li H R 2016 *Chin. Phys. B* **25** 98201
[34] Wang X, Chen H, Li C Y and Li H R 2017 *Chin. Phys. B* **26** 037105
[35] Adolphs J and Renger T 2006 *Biophys. J.* **91** 2778
[36] Kolli A, O'Reilly E J, Scholes G D and Castro O A 2012 *J. Chem. Phys.* **137** 174109
[37] Viani L, Corbella M, Curutchet C, O'Reilly E J, Castro O A and Mennucci B 2014 *Phys. Chem. Chem. Phys.* **16** 16302
[38] Aghtar M, Strümpfe J, Olbrich C, Schulten K and Kleinekathöfer U 2014 *J. Phys. Chem. Lett.* **5** 3131
[39] Rivera E, Montemayor D, Masia M and Coker D F 2013 *J. Phys. Chem. B* **117** 5510
[40] Fleming G R and Scholes G D 2004 *Nature* **431** 256
[41] Cheng Y C and Fleming G R 2009 *Ann. Rev. Phys. Chem.* **60** 241
[42] Grondelle V R and Novoderezhkin V I 2006 *Phys. Chem. Chem. Phys.* **8** 793
[43] Cui X Y, Yan Y J and Wei J H 2020 *J. Phys. Chem. B* **124** 2354
[44] Beljonne D, Curutchet C, Scholes G D and Silbey R J 2009 *J. Phys. Chem. B* **113** 6583
[45] Scholes G D 2003 *Ann. Rev. Phys. Chem.* **54** 57
[46] Sener M, Strümpfe J, Hsin J, Chandler D, Scheuring S, Hunter C N and Schulten K 2011 *Chemphyschem* **12** 518
[47] Wu J L, Silbey R J and Cao J S 2013 *Phys. Rev. Lett.* **110** 200402
[48] Cao J S and Silbey R J 2009 *J. Phys. Chem. A* **113** 13825

[49] Cleary L and Cao J S 2013 *New J. Phys.* **15** 125030
[50] Scholes G D, Fleming G R, Castro A O and Grondelle V R 2011 *Nat. Chem.* **3** 763
[51] Mallouk T E 2010 *J. Phys. Chem. Lett.* **1** 2738
[52] Curutchet C, Scholes G D, Mennucci B and Cammi R 2007 *J. Phys. Chem. B* **111** 13253
[53] Doust A B, Wilk K E, Curmi P MG and Scholes G D 2006 *J. Photochem. Photobiol. A* **184**
[54] Scholes G D, Curutchet C, Mennucci B, Cammi R and Tomasi J 2007 *J. Phys. Chem. B* **111** 6978
[55] Iozzi M F, Mennucci B, Tomasi J and Cammi R 2004 *J. Chem. Phys.* **120** 7029
[56] Yan Y J and Xu R X 2005 *Annu. Rev. Phys. Chem.* **56** 187
[57] Leggett A J, Chakravarty S, Dorsey A T, Fisher M PA, Garg A and Zwerger W 1987 *Rev. Mod. Phys.* **59**
[58] Yan Y J, Jin J S, Xu R X and Zheng X 2016 *Front. Phys.* **11** 110306
[59] Yan Y J 2014 *J. Chem. Phys.* **140** 054105
[60] Zhang H D, Xu R X, Zheng X and Yan Y J 2015 *J. Chem. Phys.* **142** 024112
[61] Cui L, Zhang H D, Zheng X, Xu R X and Yan Y J 2019 *J. Chem. Phys.* **151** 024110
[62] Zhang H D, Cui L, Gong H, Xu R X, Zheng X and Yan Y J 2020 *J. Chem. Phys.* **152** 064107
[63] Tanimura Y 1990 *Phys. Rev. A* **41** 6676
[64] Tanimura Y 2006 *J. Phys. Soc. Jpn.* **75** 082001
[65] Jin J S, Wang S K, Zheng X and Yan Y J 2015 *J. Chem. Phys.* **142** 234108
[66] Ding J J, Xu R X and Yan Y J 2012 *J. Chem. Phys.* **136** 224103
[67] Chin A W, Datta A, Caruso F, Huelga S F and Plenio M B 2010 *New J. Phys.* **12** 065002